ministered by the American Chemical Society.

†Address after September 1972: Systems, Science & Software, P. O. Box 1620, La Jolla, Calif. 92037.

[1]B. J. Alder and T. E. Wainwright, J. Chem. Phys. 33, 1439 (1960), and Phys. Rev. 127, 359 (1962).

[2]J. P. Hansen and L. Verlet, Phys. Rev. 184, 151 (1969); D. Henderson and J. A. Barker, Mol. Phys. 14, 587 (1968); H. C. Longuet-Higgens and B. Widom, Mol. Phys. 8, 549 (1964).

[3]F. Lado, J. Chem. Phys. 49, 3092 (1968).

[4]E. Thiele, J. Chem. Phys. 39, 474 (1963); M. S. Wertheim, Phys. Rev. Lett. 10, 321 (1963).

[5]J. K. Percus, in *Equilibrium Theory of Classical Fluids*, edited by H. L. Frisch and J. L. Lebowitz (Benjamin, New York, 1964), Sect. 10.

[6]H. C. Andersen and D. Chandler, to be published.

[7]Making use of the inequalities $x(1+x)^{-1} \leq \ln(1+x) \leq x$ for $x > -1$, one shows that $-p(0) \leq I \leq -p(0) - 1 - c(0)$. Condition (iv) says that $p(0)$ is finite, and conditions (i), (ii), and (iv) can be applied to prove that $-[1+c(0)]$ is bounded and positive.

[8]Equations (12a) and (12b) are derived by commuting the β differentiation with the integrations. This procedure is legitimate since conditions (ii) and (iii) imply that the integrals in Eqs. (12a) and (12b) are nonsingular for $0 \leq \beta \leq 1$.

Parametric Excitation of Electromagnetic Waves

D. W. Forslund, J. M. Kindel, and E. L. Lindman
University of California, Los Alamos Scientific Laboratory, Los Alamos, New Mexico 87544
(Received 20 March 1972; revised manuscript received 22 June 1972)

Electromagnetic waves propagating along a dc magnetic field are shown to excite parametrically decay, purely growing, modulational and beat wave instabilities. Particular attention is given to whistler parametric instabilities, including a discussion of their nonlinear development and saturation.

Considerable attention has been given in the literature to the nonlinear behavior and stability of electromagnetic waves (in particular, whistlers[1,2]), especially to explain many natural phenomena.[3] Here we point out important new nonlinear instabilities associated with whistlers and electromagnetic plasma waves. The whistler decay and purely growing instabilities, in particular, provide an important dissipation mechanism in parallel and oblique collisionless shock waves[4] such as Earth's bow shock. Because of the very low threshold in low-β plasmas, the decay instability may occur in the magnetosphere and play a role in triggered vlf emissions.

The stability analysis below, which applies to a general electromagnetic wave, also predicts new electromagnetic instabilities as well as some previously discussed[5] which can be important in laser-plasma interactions. We focus here, however, on the whistler problem, with more details of it and the laser problem to appear in a forthcoming publication.

The equilibrium considered is that of a large-amplitude circularly polarized electromagnetic wave propagating along a dc magnetic field, $\vec{B}_0 = B_0\hat{e}_x$, at a frequency ω_0 and wave number $\vec{k}_0 = k_0\hat{e}_x$ with field

$$\vec{B}_w = B_w[\hat{e}_y \cos(\omega_0 t - k_0 x) + \hat{e}_z \sin(\omega_0 t - k_0 x)].$$

The motion of a particle in this pump wave is described simply in terms of the above sinusoidal functions in the limit $k_0 v_e/\omega_0 \ll 1$,[6] where $v_e \equiv (T_e/m_e)^{1/2}$ is the thermal velocity along x.

A linear perturbation along x of the above inhomogeneous time and space equilibrium can be described completely in terms of the waves $E_n \times \exp[i(\omega + n\omega_0)t - i(k + nk_0)x]$, where $n = 0, \pm 1$. The $\omega - \omega_0$ (mode 1) and $\omega + \omega_0$ (mode 2) waves are circularly polarized electromagnetic waves such as a whistler, while the $n = 0$ wave is electrostatic such as an ion wave. For a sufficiently large pump, all three of these linear waves grow in time at the same rate at the expense of the pump field energy.

Only the results of the linear calculation are presented here. Both a fluid and an equivalent Vlasov treatment, i.e., the "$\vec{k}\cdot\Delta\vec{x}$ technique,"[6] have produced identical results in the fluid limit. In the former case, the full set of Maxwell's equations are combined with the electron's momentum and continuity equations and the ion equation of motion with only the E_0 force. For the electrons a simple scalar pressure is assumed. Dissipation effects are included phenomenologically.

The resulting dispersion relation, which is of the generic form for three-wave mode coupling problems, is

$$\epsilon_0 = (1 + \chi_I^0)(M_{11}/\epsilon_1 + M_{22}/\epsilon_2), \quad (1)$$

where

$$M_{jj}=(-\chi_e^0/2\eta_j)(\Omega_{ew}^2/\omega_{pe}^2)[(\epsilon_j-1)(\eta_0K_0-\eta_jK_j)^2+\epsilon_j\eta_0K_0(\eta_j-\eta_0)], \quad (2)$$

$$\epsilon_j=1-\bar{\omega}_j/k_j^2\eta_j(\Omega_e-\bar{\omega}_j), \quad (3)$$

$$\epsilon_0=1+\chi_I^0+\chi_e^0=1-\sum_{e,I}\frac{Z'(\bar{\omega}/2kv_j)}{2k^2\lambda_{Dj}^2}, \quad (4)$$

and where Z' is the derivative of the plasma dispersion function, Ω_{ew} is the wave gyrofrequency, $K_i\equiv ck_i/\omega_{pe}$, $\eta_j\equiv 1-\omega_j^2/c^2k_j^2$, $\eta_0\equiv 1-\omega_0^2/c^2k_0^2$, $\bar{\omega}_j=\omega_j+i\gamma_j$, with $\omega_{1,2}\equiv\omega_0\mp\omega$, $k_{1,2}\equiv k_0\mp k$, γ_j for $j=1,2$ is the damping rate, and $\bar{\omega}=\omega+i\nu$, ν being a phenomenological collisional damping rate; other definitions are standard.

The mode coupling coefficient M_{jj} results from two coupling processes which tend to reinforce each other. In the presence of the large-amplitude electromagnetic (pump) wave, a linear perturbation of the $\vec{v}\times\vec{B}$ force in the direction of $\vec{k}_0$ due to the linear electromagnetic wave drives up an electrostatic density fluctuation n_1 along $\vec{k}_0$. In turn, n_1 couples with the zero-order electron velocity to produce a first-order current perturbation $en_1\vec{v}_0$ which drives up a magnetic perturbation $\vec{B}_1$. M_{jj} is the product of these two coupling processes and thus describes how energy is coupled between a linear electromagnetic wave and density fluctuations at the expense of the pump field.

Three classes of instabilities can be identified by their behavior slightly above threshold. The decay type of instability (class I) arises when n_1 and one of the linear electromagnetic waves are driven at linear normal-mode frequencies. Another class (II) arises when both linear electromagnetic waves but not n_1 are near linear normal modes; the density fluctuations couple energy between the modes at the expense of the pump. A third class (III) exists when none of the waves are linear normal modes but instead are unstable modes created by the pump.

If the pump wave is an electromagnetic plasma wave, i.e., $\omega_0^2=\omega_{pe}^2+k_0^2c^2$, Eq. (1) contains a purely growing ion instability and a $k\sim k_0$ electron instability[7] not previously considered.[5]

When the pump is a whistler wave with $\omega_{pe}>\Omega_e$, four types of parametric instabilities exist. Figure 1 summarizes the growth rates for these instabilities for the numerical simulation parameters. The instabilities are the following:

(1) Modulational instability (class II). In the limit of $\omega\ll\omega_0$ and $k\ll k_0$, the dispersion relation of Eq. (1) agrees exactly with that of Hasegawa.[2]

(2) The beat wave instability (class II), involving only electrons. The condition that both high-frequency waves satisfy the linear whistler dispersion relation and thus be unstable requires that $K^2=3K_0^2-1$. The bandwidth of the instability, however, is only on the order of $\Omega_{ew}^2/\omega_{pe}^2$ which is 1/400 in Fig. 1. In contrast to the modulational instability, the real part of ω can be a large fraction of ω_0 and is given by $\omega/\omega_0=K/2K_0^3$, while the growth rate scales as $\omega_0\Omega_{ew}/\omega_{pe}$.

(3) Ion decay instability. The most important whistler instability over a wide range of parameters is the class I type in which the pump wave decays into a backward-going whistler at $-\vec{k}_0$ and an ion acoustic wave ω, at $2\vec{k}_0$. Near threshold the matching conditions $\omega_0=\omega_1+\omega_s$ and $\vec{k}_0=\vec{k}_1+2\vec{k}_0$ are satisifed. The electromagnetic wave ω_2 is generally negligible except when the usually small amplitude parameter $\alpha\equiv(\Omega_i/\omega_0)B_w^2/B_0^2$ is on the order of 1. Instability occurs for[8]

$$B_w^2/B_0^2>8(1+K_0^2)\beta_e\gamma_1\gamma_0/\omega_0\omega_s, \quad (5)$$

where $\omega_s=2k_0(T_e/m_i)^{1/2}$, $\beta_e=8\pi nT_e/B_0^2$, and γ_0 is the damping on the acoustic wave. Just above threshold for $\alpha^{1/3}\ll\omega_s/\omega_0$, the maximally growing wave is $\omega=\omega_s+i\omega_0(\alpha\omega_0/\omega_s)^{1/2}$. For $\alpha^{1/3}\gg\omega_s/$

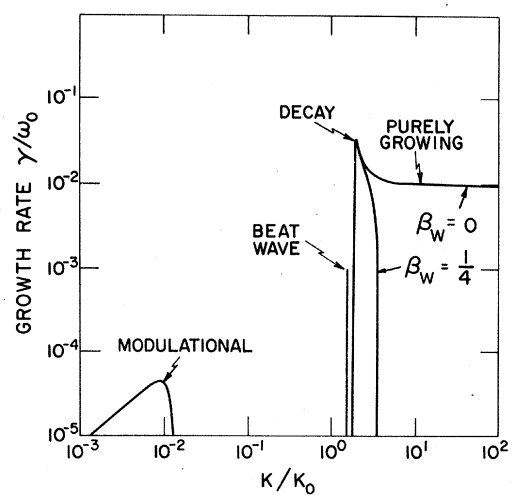

FIG. 1. Solutions to Eq. (1) for $B_w/B_0=0.2$, $\omega_{pe}/\Omega_e=4$, $M_i/m_e=1836$, $K_0=\pi/2$, $\omega_0/\Omega_e=0.71$, and $\beta_w=0,\frac{1}{4}$, illustrating the four basic instabilities.

ω_0, the most unstable wave is

$$\omega/\omega_0 = \tfrac{1}{2}(2\alpha)^{1/3}(1+i\sqrt{3}). \quad (6)$$

In Fig. 1 the decay instability region occupies a narrow bandwidth ($\sim \alpha^{1/3}$) around $2k_0$ with the maximum growth rate described by Eq. (6).

(4) Purely growing ion instability. For $k > 2k_0$ the decay instability changes into this class III instability with nearly zero real frequency when damping is negligible. In the fluid acoustic limit the frequency is

$$\omega = ikv_A \frac{B_w}{B_0}\left(\frac{k_0^2}{k^2-4k_0^2} - \frac{\beta_w}{2}\right)^{1/2}, \quad (7)$$

where $\beta_w = 8\pi n T_e/B_w^2$ and v_A is the ion Alfvén speed. The growth rates are largest near the decay instability resonance, and the high-k cutoff is just the Bennett pinch condition[9] aided by this resonance.

The results of a one-dimensional numerical simulation[10] with the parameters of Fig. 1 which primarily emphasized the whistler decay instability are shown in Figs. 2 and 3. In Fig. 2 "B_k^2 Left" is a plot near saturation of the spatially circularly polarized magnetic field B_k^2 as a function of k in the direction of the large-amplitude whistler. The two largest waves are the pump at mode 2 and another whistler at $k = 3k_0$ (the $k + k_0$ mode) whose energy is about 10^{-3} of the driver. For "B_k^2 Right," which is the Fourier plot for negative wave numbers, i.e,, the opposite spatial polarization, there is a sharp peak at the second mode, i.e., $-k_0$, corresponding to the decay instability into a whistler moving opposite to the driver. The energy in mode 3 ($-1.5k_0$) occurs because of the excitation of the purely growing mode. The electrostatic field energy E_k^2 is plotted as a function of k in the third portion of Fig. 2; it shows a peak due to the ion wave at mode 4 or $k = 2k_0$ with no corresponding peak in the magnetic field energy. The whistlers at $k = -k_0$ and $k = 3k_0$ and the ion wave at $k = 2k_0$ correspond to the unstable three-component eigenmode. The growth rate of the three components follows Eq. (6) to within 10% and the relative amplitudes agree with a calculation of the eigencomponents.

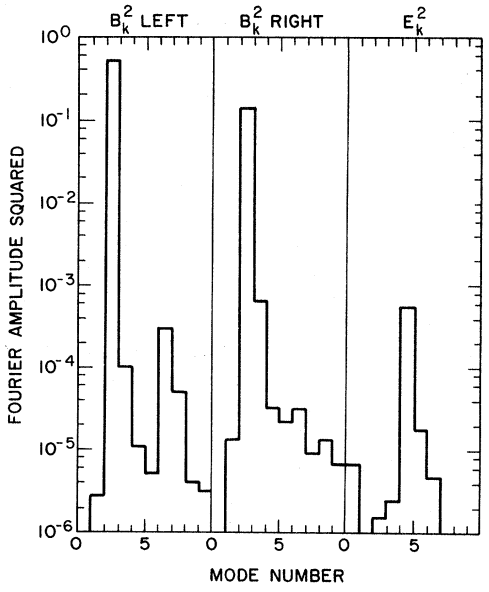

FIG. 2. Fourier amplitudes of the two spatial polarizations of the magnetic field and the electrostatic field at $T = 1000\omega_{pe}^{-1}$ for a simulation with the parameters of Fig. 1 ($\beta_w = \frac{1}{4}$) and $T_e/T_i = 25$, a system length of $8c/\omega_{pe}$, 20 000 simulation particles, cell size $\sim v_e/\omega_{pe}$, and timestep $0.2\omega_{pe}^{-1}$.

There are three basic mechanisms which can alter or stop the linear growth of the decay and purely growing instability.

(A) Saturation by 100% modulation. Unless the parameter $\alpha \sim 1$, saturation of the decay instability occurs when the backward traveling whistler becomes equal in amplitude to the pump wave, thus saturating the mode coupling. The plot of B_y versus B_z with x as a parameter in Fig. 3(c) illustrates both the initial circular polarization of the driving whistler and the net linear spatial polarization at saturation corresponding to 100% modulation as shown by the amplitude of B in Fig. 3(f).

(B) Saturation by ion wave breaking. At high pump field ($\alpha \sim 1$) linear growth may terminate by the breaking of the excited ion wave. Since the mode coupling is not stopped, however, it ap-

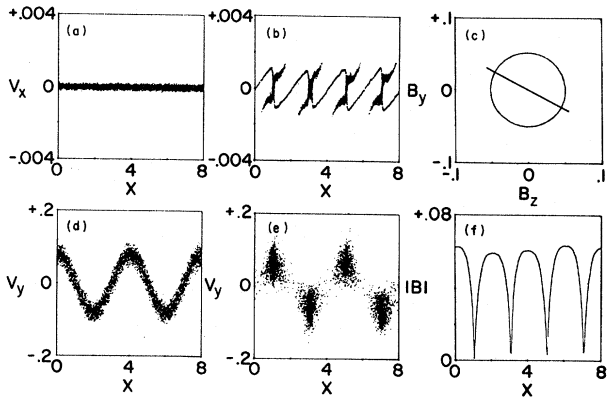

FIG. 3. (a), (d) Particle phase-space and magnetic field plots for the simulation at $T = 0$; (b), (c), (e), (f) at $T = 2000\omega_{pe}^{-1}$.

pears to be only a quasisaturation, reducing the rate of equilibration of pump and wave energies. Two types of breaking are observed to occur: (a) the usual ion trapping mechanism in acoustic waves when the wave amplitude is large enough for the ion trapping velocity to equal the (complex) phase velocity of the wave, and (b) higher-order mode coupling which causes the ion wave to steepen and adds to the ion trapping distortion of the wave. Wave breaking occurs at much higher amplitude than in the usual ion-acoustic wave because the pump wave has increased the phase velocity much above the acoustic speed [cf. Eq. (6)]. The ion wave field at breaking of type (a) can be related to the backward-traveling whistler amplitude from the eigenvector equation used to determine the dispersion relation. This determines a critical whistler amplitude B_{1c} at which breaking occurs, $B_w/B_{1c} \approx 4\alpha^{1/3}(1+K_0^2)$. If $B_w/B_{1c} < 1$, ion breaking cannot occur before 100% modulation; whereas if $B_w/B_{1c} > 1$, it can.

A comparison of the intial ion v_x-x phase space of Fig. 3(a) with that at $T = 2000\omega_{pe}^{-1}$ in Fig. 3(b) shows the development of the large-amplitude ion wave and the associated strong ion trapping. The trapping observed is of the type (b) and occurs shortly after the saturation by 100% modulation since $B_w/B_{1c} \sim \frac{1}{3}$. The ion kinetic energy in the ion wave in the linear regime, which is $(B_w/8B_{1c})B_1^2/8\pi$, provides a reasonable estimate of the ion heating at breaking.

(C) Saturation by electron heating. As shown in Fig. 1 and in Eq. (7), finite electron pressure stabilizes the short-wavelength purely growing mode. However, electron pressure has little effect on the decay instability. A comparison of the initial equilibrium electron v_y-x phase space in Fig. 2(d) with that at $T = 2000\omega_{pe}^{-1}$ in Fig. 2(c) shows the strong clumping of the electron currents associated with the ion density peaks of the ion wave. Very little electron heating is observed, however, because the initial $\beta_w = \frac{1}{4}$ stabilizes almost all the purely growing modes. Other simulations with colder electrons shows strong electron heating until $\beta_w \sim \frac{1}{4} - \frac{1}{2}$.

Simulations of high-Mach-number switch-on shocks have also shown clear evidence of these decay and purely growing instabilities. Since the whistlers in these shocks have $\alpha \sim 1$ and, hence, parametric growth rates $\gamma \sim \omega_0$, even relatively short whistler wave trains in front of the shock will be very strongly unstable. The short-wavelength, purely growing instability tends to heat the electrons until $\beta_e \sim 1$ behind the shock, while the decay instability causes strong ion heating and, hence, a highly turbulent shock structure.[4] Although the equilibrium is more complicated, we expect the parametric instabilities to persist in the oblique whistler problem although in a modified form[11] and provide the explanation of the shock structures observed by Biskamp and Welter.[4]

This work was performed under the auspices of the United States Atomic Energy Commission.

[1]R. F. Lutomirski and R. N. Sudan, Phys. Rev. 147, 156 (1966); T. Taniuti and H. Washimi, Phys. Rev. Lett. 22, 454 (1969); R. Prasad, Phys. Fluids 13, 1310 (1970).

[2]A. Hasegawa, Phys. Fluids 15, 870 (1972).

[3]R. A. Helliwell, J. Geophys. Res. 72, 4773 (1967), and many other articles by this author; R. N. Sudan and E. Ott, J. Geophys. Res. 76, 4773 (1971), and references therein; K. B. Dysthe, J. Geophys. Res. 76, 6915 (1971), and references therein, especially those by K. F. Harker and F. W. Crawford.

[4]D. Biskamp and H. Welter, Phys. Rev. Lett. 28, 410 (1972).

[5]Y. R. Shen and N. Bloembergen, Phys. Rev. 137, A1787 (1965); S. E. Bodner and J. L. Eddleman, Lawrence Livermore Laboratory Report No. 73378, 1971 (unpublished); M. Bornatici, A. Cavaliere, and F. Engelmann, Phys. Fluids 12, 2362 (1969).

[6]Y. C. Lee and P. K. Kaw, Phys. Fluids, 15, 911 (1972).

[7]C. Max and F. Berkins (private communication) have independently found an electron instability for k near k_0. For a relativistic treatment where $k_0 = 0$, see C. Max and F. Perkins, in *Proceedings of a Symposium on Anomalous Absorption of Intense Radiation, Boulder, Colorado, 1972* (unpublished).

[8]K. Nishikawa, J. Phys. Soc. Jap. 24, 916 (1968).

[9]H. P. Furth, Phys. Fluids 6, 48 (1963).

[10]R. L. Morse and C. W. Nielson, Phys. Fluids 14, 830 (1971).

[11]J. M. Kindel, H. Okuda, and J. M. Dawson (to be published) have examined the very oblique problem in the electrostatic approximation.